

## Durham Research Online

---

### Deposited in DRO:

23 September 2016

### Version of attached file:

Published Version

### Peer-review status of attached file:

Peer-reviewed

### Citation for published item:

Šibalić, N. and Kondo, J.M. and Adams, C.S. and Weatherill, K.J. (2016) 'Dressed-state electromagnetically induced transparency for light storage in uniform-phase spin waves.', *Physical review A.*, 94 (3). 033840.

### Further information on publisher's website:

<http://dx.doi.org/10.1103/PhysRevA.94.033840>

### Publisher's copyright statement:

This article is available under the terms of the Creative Commons Attribution 3.0 License. Further distribution of this work must maintain attribution to the author(s) and the published article's title, journal citation, and DOI.

### Additional information:

## Use policy

---

The full-text may be used and/or reproduced, and given to third parties in any format or medium, without prior permission or charge, for personal research or study, educational, or not-for-profit purposes provided that:

- a full bibliographic reference is made to the original source
- a [link](#) is made to the metadata record in DRO
- the full-text is not changed in any way

The full-text must not be sold in any format or medium without the formal permission of the copyright holders.

Please consult the [full DRO policy](#) for further details.

# Dressed-state electromagnetically induced transparency for light storage in uniform-phase spin waves

N. Šibalić,<sup>\*</sup> J. M. Kondo,<sup>†</sup> C. S. Adams, and K. J. Weatherill

*Joint Quantum Center (JQC) Durham-Newcastle, Department of Physics, Durham University,  
South Road, Durham DH1 3LE, United Kingdom*

(Received 27 July 2016; published 21 September 2016)

We present, experimentally and theoretically, a scheme for dressed-state electromagnetically induced transparency (EIT) in a three-step cascade system in which a four-level system is mapped into an effective three-level system. Theoretical analysis reveals that the scheme provides coherent-state control via adiabatic following and a generalized protocol for light storage in uniform phase spin-waves that are insensitive to motional dephasing. The three-step driving enables a number of other features, including spatial selectivity of the excitation region within the atomic medium, and kick-free and Doppler-free excitation that produces narrow resonances in thermal vapor. As a proof of concept, we present an experimental demonstration of the generalized EIT scheme using the  $6S_{1/2} \rightarrow 6P_{3/2} \rightarrow 7S_{1/2} \rightarrow 8P_{1/2}$  excitation path in thermal cesium vapor. This technique could be applied to cold and thermal ensembles to enable longer storage times for Rydberg polaritons.

DOI: [10.1103/PhysRevA.94.033840](https://doi.org/10.1103/PhysRevA.94.033840)

## I. INTRODUCTION

The coherent mapping of light fields into excitations of matter [1] is a key feature of the storage and manipulation of optical quantum information [2]. Atomic media have significant appeal because they provide inherently narrow and well-defined optical transitions [3], and they are matched to vapor-based single-photon sources. Light fields can be compressed inside a medium by using highly dispersive transparency windows formed using electromagnetically induced transparency (EIT) [4,5], and then they can be coherently mapped as atomic excitation through adiabatic following [1]. Furthermore, the mapping of coherence between an atomic ground state and a Rydberg (highly excited) state allows manipulations at the single-photon level [6] because strong atom-atom interactions lead to very large optical nonlinearities [7,8] producing effective photon-photon interactions that can be used for nonclassical light generation [9,10] and quantum gate protocols [11,12]. However, excitation of Rydberg states typically requires ladder excitation schemes, which produce stored states that are sensitive to atomic motion due to mismatched wave vectors of the excitation lasers.

Atomic motion in atom-based light memories reduces retrieval efficiency, since spatial selectivity of the readout channel depends crucially on the constructive interference of contributions from the initially stored spin-wave. This collectively stored excitation inherits its relative phase from the laser beams, with respective wave vectors  $\mathbf{k}_i$ , used in the storage protocol [13]. In particular, in ladder excitation

schemes, such as those used for Rydberg states [14], typically there is a large wave-vector mismatch, i.e.,  $|\sum \mathbf{k}_i| \equiv 2\pi/\Lambda \neq 0$ , which causes oscillations in the relative phase of the excited medium with a spatial period of  $\Lambda$ . The thermal motion of the atoms causes the imprinted spin-wave phase grating to diffuse [13,15], reducing the visibility of the interference pattern that selects the preferential output direction. This effect limits the maximum storage times and minimum dephasing rate for coherent manipulation [13,16–18].

Here we propose an approach to writing uniform-phase spin-waves, based on a Doppler-free three-photon ladder excitation scheme. With three driving fields oriented in a plane such that the wave vectors cancel, i.e.,  $\sum \mathbf{k}_i = \mathbf{0}$ , each atom picks up the same phase, independent of their spatial position. Therefore, the spin-wave written into the highly excited state is insensitive to motional dephasing. In addition, we show that typical two-photon storage protocols can be easily mapped to the four-level schemes, allowing coherent manipulation. The combination of Doppler-free excitation of Rydberg states into collective excitation with uniform phase, and the coherent control of atom populations via adiabatic following, highlights some fundamental advantages of three-photon coherent excitation over conventional two-photon schemes.

The paper is organized as follows. In Sec. II we introduce the idea of using EIT occurring due to the destructive interference of two excitation paths over a dressed state excited in a Doppler-free configuration. Subsequently, we discuss the important aspects of this scheme for both thermal and cold-atom ensembles. In Sec. III we discuss the scheme as a way of storing light as collective atomic excitation, forming a spin-wave with a uniform phase. We discuss the prolonged storage time and consequences of purifying the readout state down to the single-photon level. In Sec. IV we show how one can easily generalize well-known two-photon protocols for light storage through adiabatic following over a dressed state. In Sec. V we discuss the benefits of spatial selectivity afforded by the proposed scheme. Section VI presents a proof-of-principle experimental demonstration of four-level dressed-state EIT in thermal vapor under Doppler-free conditions. Finally, we present conclusions and an outlook in Sec. VII.

<sup>\*</sup>nikolasibalic@physics.org

<sup>†</sup>Present address: Departamento de Física, Universidade Federal de Santa Catarina, Campus Trindade, Florianópolis 88040-900, SC, Brazil.

*Published by the American Physical Society under the terms of the Creative Commons Attribution 3.0 License. Further distribution of this work must maintain attribution to the author(s) and the published article's title, journal citation, and DOI.*

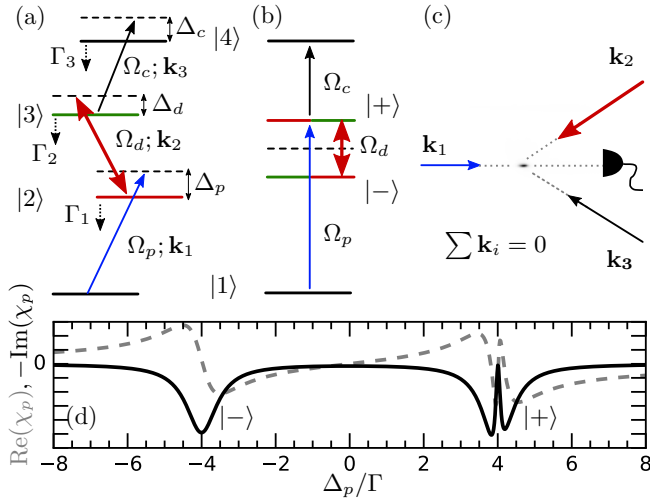


FIG. 1. (a) Level diagram for bare states in a four-level ladder scheme. (b) Levels in the semidressed state picture. (c) Three beams are oriented in a plane in the Doppler-free configuration. With both probe and control lasers detuned from bare-state resonance, strong atom-light interactions occur only in the common focus of all three beams. (d) Theoretical calculation of the real (dashed) and imaginary (solid) parts of the electric susceptibility around the probe transition resonance frequency with parameters  $\Gamma_1 = \Gamma_2 = \Gamma$ ,  $\Gamma_3 = 0$ ,  $(\Omega_d, \Omega_p, \Omega_c)/\Gamma = (8, 0.1, 0.5)$ , and  $(\Delta_d, \Delta_c)/\Gamma = (0, -4)$  for a stationary four-level atom.

## II. EIT USING AN ENGINEERED STATE

We consider a four-level ladder system [Fig. 1(a)] driven by three coherent fields (denoted probe, dressing, and control) with the corresponding Rabi driving frequencies  $\Omega_p, \Omega_d$ , and  $\Omega_c$ , and the corresponding detunings of the individual lasers of  $\Delta_p, \Delta_d$ , and  $\Delta_c$  [Fig. 1(a)], as described by the Hamiltonian in the  $(|1\rangle, \dots, |4\rangle)$  basis ( $\hbar = 1$ ),

$$\mathcal{H} = \begin{pmatrix} 0 & \Omega_p/2 & 0 & 0 \\ \Omega_p/2 & -\Delta_p & \Omega_d/2 & 0 \\ 0 & \Omega_d/2 & -\Delta_p - \Delta_d & \Omega_c/2 \\ 0 & 0 & \Omega_c/2 & -\Delta_p - \Delta_d - \Delta_c \end{pmatrix}. \quad (1)$$

In addition to the coherent driving, dissipation affecting the system is described by the Lindblad superoperator acting on the density matrix  $\hat{\rho}$  of the system  $\mathcal{L}[\hat{\rho}] = \sum_k (L_k \hat{\rho} L_k^\dagger - \frac{1}{2} L_k^\dagger L_k \hat{\rho} - \frac{1}{2} \hat{\rho} L_k^\dagger L_k)$ , where we include spontaneous decays with rates  $\Gamma_1, \dots, \Gamma_3$ ,  $L_1 = \sqrt{\Gamma_1}|0\rangle\langle 1|$ ,  $L_2 = \sqrt{\Gamma_2}|1\rangle\langle 2|$ ,  $L_3 = \sqrt{\Gamma_3}|2\rangle\langle 3|$ . The system dynamics is governed by the master equation  $\dot{\hat{\rho}} = -i[\mathcal{H}, \hat{\rho}] + \mathcal{L}[\hat{\rho}]$ .

We focus our attention on the parameter regime where the middle-step laser, resonant with the unperturbed transition  $|2\rangle \rightarrow |3\rangle$ ,  $\Delta_d = 0$ , introduces a strong dressing,  $\Omega_d \gg \Omega_p, \Omega_c$ , of the two intermediate states. The goal is to carry out Autler-Townes splitting of the resonance from the ground state, as illustrated in Fig. 1(d). The probe and coupling laser fields are both *detuned from the bare-state resonances* ( $\Delta_p = -\Delta_c = \Omega_d/2$ ) so that they fulfill the condition for resonance for one of the dressed states  $|+\rangle$  or  $|-\rangle$  [Fig. 1(b)]. This engineered state can be used in combination with a strong

control  $\Omega_c$  and weak probe  $\Omega_p$  to open a narrow transparency window for the probe light [Fig. 1(d)]. We consider the typical situation in which the Rydberg state  $|4\rangle$  decay is much weaker compared to that of the intermediate states  $\Gamma_3 \ll \Gamma_1 \approx \Gamma_2$ . To a very good approximation a dark state  $|D\rangle$  is formed, which can be obtained from Eq. (1) for the limiting worst case of  $\Omega_p = \Omega_c$  in the form

$$|D\rangle = (|1\rangle - \varepsilon|2\rangle - \varepsilon|3\rangle + |4\rangle)/N, \\ \varepsilon \equiv \frac{-\Omega_d + \sqrt{\Omega_c^2 + \Omega_d^2}}{\Omega_c},$$

where  $N$  is the normalization factor, and  $\varepsilon$  characterizes the amount of the admixture of the bright (radiatively coupled) states  $|2\rangle$  and  $|3\rangle$ . We see that in the limit of strong dressing, the contribution of the bright states  $2\varepsilon \sim \Omega_c/\Omega_d \ll 1$  is negligible. This is similar to the double-dark resonance scheme used in  $\Lambda$  systems [19]. However, the benefit of using the engineered state for excitation becomes apparent if one considers momentum kick-free, Doppler-free excitation. While typical two-photon driving to highly excited states cannot fulfill the Doppler-free conditions due to mismatch in the excitation laser wavelengths, this is easily done with three driving fields arranged in a plane [Fig. 1(c)], further advantages of which will be discussed in the following section.

We note that the dressed-state EIT approach can be extended to more complicated multilevel cascade excitation schemes, following the same principle by which the probe and the coupling laser are detuned from bare-states resonances, so that they are resonant with one of the engineered states that appear in the semidressed picture of the strong resonant dressing of the intermediate levels. This makes it possible to use new level schemes for engineering interactions between multiple polaritons. However, this will not be considered further in this work.

## III. UNIFORM PHASE SPIN-WAVE

Doppler-free excitation offers additional advantages for atomic memories based on collective superpositions of stored excitations [1,20]. Whenever a photon from the probe field is stored as an excitation of the Rydberg state, the atomic excitation picks up a phase from three laser beams. For the Doppler-free configuration of beams with wave vectors  $\mathbf{k}_i$ , the phase of the excitation is independent of the position  $\mathbf{r}$  of the excitation in the cloud since  $\sum \mathbf{k}_i \cdot \mathbf{r} = 0$ . Since the phase grating determining the output mode will now be determined only by the readout beams, any atomic motion during the storage time does not affect the retrieval efficiency [21]. Also, the output mode *direction* can be changed, while maintaining the encoded quantum information, by using a different alignment of the output lasers. Similarly, the readout *frequency* can be changed by using a different dressed state for the readout [22]. These features could be important for realizing quantum interconnects [2].

A prominent example in which the increase in storage lifetime can have an impact is the Rydberg-vapor based single-photon source [23]. Recent storage times with light stored as Rydberg excitation in thermal vapor yield the lifetime of the memory of only about 1.2 ns [24], limited by

atomic-motion-induced dephasing of the spin-wave imprinted by the two-photon excitation. With the proposed Doppler-free excitation, the lifetime of this atom vapor memory would be limited by the transit time of atoms through the interaction region. For example, for Rb at 140 °C and a laser beam waist of 35  $\mu\text{m}$  as in Ref. [24], a lifetime that is two orders of magnitude higher is expected. The longer storage time would also increase effectively the blockaded volume. To obtain single photons from the output, one usually relies on a strong blockade, assuming that multiple excitations will dephase on the time scale of the excitation laser pulse [23,24] due to atom interactions causing level shifts of  $C_\alpha/r^\alpha$  for atoms at a distance  $r$  interacting with resonant dipole-dipole ( $\alpha = 3$ ) or off-resonant van der Waals ( $\alpha = 6$ ) interactions, where constant  $C_\alpha$  is characteristic of the excited state. This requires small excitation volumes in order to achieve strong enough interactions. The longer lifetime, which is achievable in principle with uniform-phase spin-wave storage, can be used for cleaning the multiphoton output from the output mode after the storage of the initial pulse, since interactions will dephase the spin-waves containing multiple excitations [25], preventing their readout in the output mode. For clouds of size  $l$ , this decoupling of the multiphoton excitations from the output mode would happen after  $\sim l^\alpha/(C_\alpha h)$ , where  $\alpha = 3$  or 6 depending on whether the Rydberg states are interacting via resonant dipole-dipole interactions or van der Waals interactions. For example, if the excitation is performed in 1 ns, waiting for a time of 100 ns would increase the excitation volume from which we still expect to get only single-photon output by factor of 100 and 10 for dipole-dipole and van der Waals interactions, respectively, corresponding to the increased effective blockade radius by a factor of 4.6 and 2.1, respectively.

#### IV. COHERENT CONTROL

In addition to achieving uniform phase spin-wave excitation, for wider application of the three-photon ladder scheme, coherent manipulation protocols allowing deterministic storage and retrieval [1] are desirable. In the previous section, we considered just stochastic excitation. For deterministic, coherent control of populations, off-resonant Doppler-free driving schemes have been proposed [26], however achieving high Rabi driving frequencies is difficult in situations with weak dipole-matrix elements and large detunings. Also, this protocol demands precise control of driving power and timing.

Adiabatic following methods offer a good alternative, relaxing the constraints on precise timing and power, yet allowing deterministic atomic state preparation, as well as mapping of weak quantum fields into atomic excitation of the medium. The standard two-photon STIRAP protocol has been used to prepare atoms in Rydberg states [27], and it can be easily generalized for usage over the engineered state. Details of the protocol are shown in the inset of Fig. 2. Keeping the dressing laser constantly on, and pulsing the control and the probe laser beams, transfers population between the ground and the Rydberg state (Fig. 2) without populating significantly any of the *two* intermediate states. Two requirements have to be satisfied for efficient transfer: (i) the dressing driving should be stronger than the probe or control driving ( $\Omega_d \gg \Omega_c, \Omega_p$ )

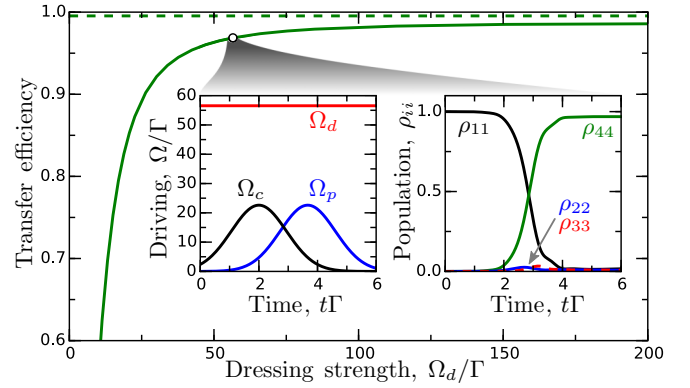


FIG. 2. Transfer efficiency to excited state  $|4\rangle$  (solid line), compared to that of the three-level scheme (dashed line) for the same control pulses. High efficiency is achieved with strong dressing of the two middle states with the generalized STIRAP protocol for a four-level ladder scheme (see the inset). States  $|1\rangle$  and  $|4\rangle$  are assumed to be long-lived, while the decay constant of each of the two middle states is  $\Gamma$ .

[28]; and (ii) the usual three-level STIRAP adiabaticity condition should be satisfied,  $\Gamma/(T\Omega^2) \ll 1$  [29], where  $\Omega$  is the control ( $\Omega_p, \Omega_c$ ) pulse intensity,  $\Gamma$  decay is the constant of the two middle (dressed) states, and  $T$  is the characteristic switching time of the two pulses.

The combination of adiabatic following and the existence of a narrow transparency window, allowing pulse slowing down and compression (Sec. II), suggest that the scheme can be used as a simple generalization of three-level storage protocols [1], offering the above-discussed benefits of uniform-phase spin-wave excitation (Sec. III). In the limit where multiple Rydberg atoms are excited at distances shorter than their characteristic interaction strength, the protocol can be used for testing proposals that exploit Rydberg-Rydberg interactions in small excitation volumes for state preparation [30]. Finally, note that the described adiabatic following protocol is only efficient for cold atoms, since in hot atoms the Doppler effect dephases the system during the adiabatic following, significantly reducing the transfer efficiency.

#### V. SPATIAL SELECTIVITY

In addition to Doppler-free excitation, the noncollinear orientation of the three beams provides an excitation volume whose size is determined by the overlap of all three beams. Since both probe and coupling beams are detuned from bare-state resonance, the medium is *transparent* for the beams everywhere except on the overlap region, which is the only place where the population of the atoms in the Rydberg or the ground state is changed. The off-resonant, noncollinear, multiphoton excitation scheme [Fig. 1(c)] allows excitation and probing of well-localized regions in any arbitrary location within the atomic medium, whose size can be down to the order of several micrometers if all the beams are tightly focused.

The excitation of atomic vapors confined in spectroscopic cells in this scheme, in combination with narrow Doppler-free features, is promising for electrometry in the microwave (MW) and terahertz (THz) domains [31,32], allowing subwavelength



imaging of fields in the vicinity of structures that are either immersed in the atomic vapor or placed next to the spectroscopic cell [33]. The scheme can also provide good spatial resolution for probing atom-surface interactions [34] for patterned surfaces inserted in the vapor cell [35], and for exploring nonequilibrium phase transitions [36] in small volumes.

In cold-atom ensembles, this excitation scheme allows exciting only a fraction of the atomic cloud, which can be important, e.g., in Rydberg experiments where one might want to perform excitation within the micrometer range characteristic for a Rydberg blockade [6,30], within the larger cold-atom clouds for state preparation [30] or for single-ion source creation [37]. Similarly, the scheme can be used for single-site addressing [38–42] in two-dimensional (2D) and 3D lattices. If the excitation is done for an atomic ensemble held in a 2D lattice, the addressing can be done only by moving the dressing laser focus, keeping wide probe and coupling beams, which illuminate the whole lattice, unchanged.

## VI. EXPERIMENTAL DEMONSTRATION OF DRESSED-STATE EIT

As a proof of concept, we provide a demonstration of the proposed EIT scheme in cesium vapor using the  $6S_{1/2}F=4 \rightarrow 6P_{3/2}F=5 \rightarrow 7S_{1/2}F=4 \rightarrow 8P_{1/2}F=3,4$  ladder scheme, with corresponding wavelengths 852, 1470, and 1394 nm, respectively. The first two lasers can be locked on resonance using Doppler-free polarization spectroscopy [43,44], while the third control laser (Qphotonics QDMLD-1392-10) is not actively stabilized. The weak probe beam, set  $2\pi \times 500$  MHz off-resonance from the transition, is obtained using an acousto-optic modulator in a double-pass configuration. The experiment is performed in a 2-mm-long quartz vapor cell (Fig. 3) containing cesium vapor at a temperature of 50 °C. All three beams are focused [beam  $1/e^2$  waists  $(w_p, w_d, w_c) = (6, 28, 29) \mu\text{m}$ ] at a common spot inside the cell. To achieve the Doppler-free configuration, dressing and control beams are focused through the 1.25-mm-thick quartz windows at an angle of 34° and 32°, respectively, to the direction of the propagation of the probe laser beam, which is incident normal to the cell windows. The astigmatism introduced by the windows offsets the foci in sagittal and tangential planes, of both dressing and control beams, by about  $\sim 0.2$  mm. This is compensated by adding additional quartz windows (AC1 and AC2 in Fig. 3) of the same thickness and at the same incident angle, but now in a sagittal plane, i.e., rotated 90° around the propagation direction with respect to the glass window.

A theoretical prediction of the probe absorption, excluding the hyperfine splitting, is presented in Fig. 4(a). The steady-state dynamics for the model in Sec. II is calculated for the ensemble of four-level atoms, taking into account Doppler broadening (at 50 °C) due to the motion of the atoms in the plane defined by the excitation lasers. Decay rates of the excited states  $\Gamma_{1,\dots,3}$  correspond to the natural lifetimes of  $6P_{3/2}$ ,  $7S_{1/2}$ , and  $8P_{1/2}$ , respectively. Additionally, each of the states decays to the ground state with the rate  $\Gamma_\tau = 1/\tau$  due to the finite transit time  $\tau$  of the atoms through the excitation region. The transparency peak that opens on one of the dressed

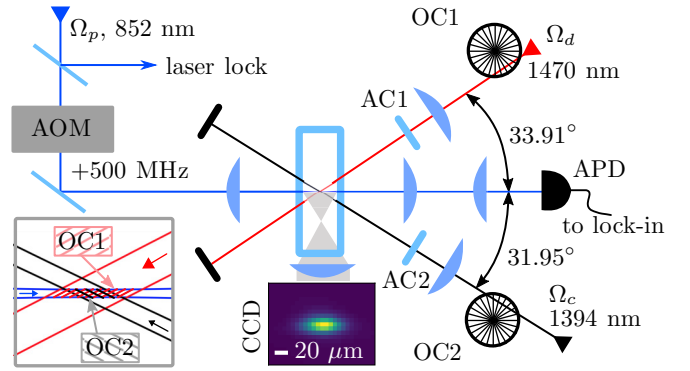


FIG. 3. Schematic of the experimental setup. An acousto-optic modulator (AOM) provides the frequency offset to the probe beam whose transmission through a 2 mm cesium vapor cell is recorded on an avalanche photodiode (APD). Dressing (1470 nm) and control (1394 nm) beams are passed through achromatic lenses and astigmatism correction plates (AC1 and AC2) before reaching a common focus inside the cell. In the combined focus, the frequency-shifted probe field becomes resonant with the transition, which causes strong 852 nm fluorescence that is imaged on the camera (CCD) from the side of the cell. The dynamics within the spot region can be extracted cleanly by performing lock-in detection with one of the optical choppers (OC1 and OC2). The inset on the bottom left shows different interaction regions from which the dynamics is extracted with corresponding optical choppers.

states  $[|+\rangle]$  in Fig. 4(a)] is limited now in visibility by the transit time.

Experimentally obtained level splitting, with the dressing laser beam ( $P_d = 4.1$  mW) on  $6P_{3/2}F=5 \rightarrow 7S_{1/2}F=4$  resonance and the control beam set off-resonance, is presented in Figs. 4(b)–4(d). An avalanche photodiode (APD) records the probe beam ( $P_p = 400$  nW) absorption [Fig. 4(b), dotted line] through the 2-mm-thick vapor region, which includes an  $\sim 10^2$  times shorter common interaction region. In the interaction region, a dressing beam induces Autler-Townes (AT) splitting of the  $6P_{3/2} \rightarrow 7S_{1/2}$  resonance, which additionally broadens the wings of the Doppler-broadened D2 spectrum. The dressing beam can be switched on and off with an optical chopper (OC1 in Fig. 3). When the APD signal is demodulated with the lock-in amplifier, we can obtain the change of probe transmission  $\delta T$  due to the dressing beam in the common interaction region. This reveals two AT peaks [Fig. 4(b), dashed line], the red-detuned one being smaller due to the contribution of other hyperfine states ( $F=3,4$ ) of the D2 line. The increased transparency when the probe is on resonance is also explained in the dressing picture, with resonance being shifted away from the probe transition due to AT line splitting. Finally, adding the control laser ( $P_c = 8.8$  mW) causes a transparency peak to appear when the resonance condition with either of the dressed states ( $|+\rangle$  or  $|-\rangle$ ) is achieved [solid line in Figs. 4(b) and 4(d)]. With maximum absorption in a demodulated signal normalized to 1 for maximum absorption, we see that we achieve transparency of  $\sim 30\%$ . Two peaks are observed, corresponding to two hyperfine states  $8P_{1/2}F=3,4$  of the final state, split by  $2\pi \times 171$  MHz. Note that if the control laser is left on resonance, enhanced absorption is observed [Fig. 4(c), solid line], which is explained as the usual

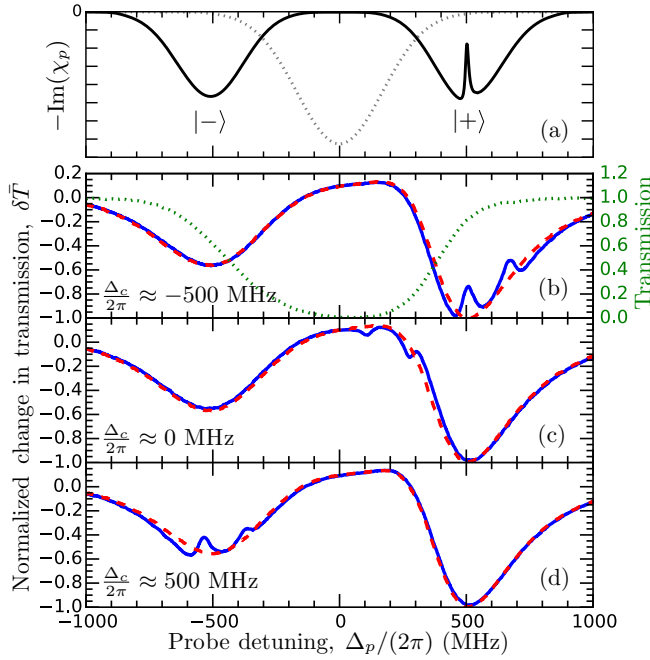


FIG. 4. (a) Four-level theoretical calculation of the imaginary part of the electric susceptibility for the Doppler-broadened medium: The dotted (solid) line shows the line profile without (with) a dressing laser beam  $\Omega_d = 0$  ( $\Omega_d = 2\pi \times 1$  GHz). The solid line shows EIT over one of the dressed states for  $\Delta_d = 0$ ,  $\Delta_c = -2\pi \times 500$  MHz for a transit lifetime of  $\tau = 26$  ns,  $(\Omega_p, \Omega_c)/(2\pi) = (1, 80)$  MHz. (b)–(d) Experiment in Cs thermal vapor: The dotted line shows the total probe transmission through the cell. Lock-in detection with modulation on the dressing beam shows AT splitting (dashed line). Addition of the control laser (solid line) opens a transparency window when the control field is detuned to one of the dressed states (b) and (d). With the control laser on resonance, EIA is observed (c).

three-photon electromagnetically induced absorption (EIA) [44–46].

To get further insight into the nature of observed EIT resonances, we now scan the control laser, leaving the probe laser locked, with the probe beam tuned  $2\pi \times 500$  MHz to the blue off resonance,  $6S_{1/2}F = 4 \rightarrow 6P_{3/2}F = 5$ , and the dressing laser locked on resonance,  $6P_{3/2}F = 5 \rightarrow 7S_{1/2}F = 4$ . Now the control laser power is modulated with the optical chopper OC2 (Fig. 3), while the dressing beam power is kept constant. Note that with this modulation, one probes, in principle, a different spatial part of the interaction region (Fig. 3, inset), although in the present case the two regions are almost the same since  $w_d \approx w_c$ . The lock-in amplifier demodulated probe absorption signal is presented in Fig. 5(a). Analysis of the resonance (marked with a dot) full width at half-maximum (FWHM) extracted from the Gaussian fits, reveals a linear scaling [Fig. 5(b)] in accordance with the theory [47]. The narrowest features in the limit of  $\Omega_c \rightarrow 0$  are about  $2\pi \times 36$  MHz. A similar analysis with unlocked lasers, and the probe on resonance  $\Delta_p \approx 0$ , yields a minimum EIA linewidth of about  $2\pi \times 29$  MHz [Figs. 5(c) and 5(d)]. These linewidths are limited by two factors: (i) the finite time the atoms spent in the interaction region, estimated as a time of flight through the probe beam, that broadens every transition

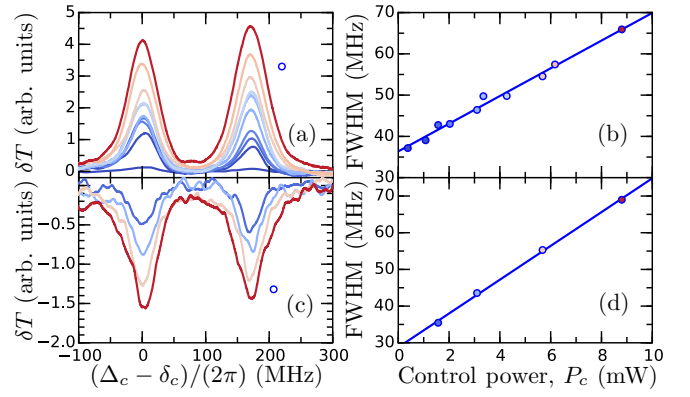


FIG. 5. EIT and EIA under conditions of strong resonant dressing  $\Delta_d = 2\pi \times 0$  MHz,  $\Omega_d = 2\pi \times 1$  GHz. (a) EIT features obtained for off-resonant probe and control  $\Delta_p = -\delta_c = 2\pi \times 500$  MHz. (b) The FWHM of EIT varies linearly with control power. (c) EIA features are observed when probe and control fields are resonant with bare state transitions  $\Delta_p = -\delta_c \approx 0$ . (d) The FWHM has linear scaling with control power.

by  $\Gamma_t = \bar{v}/\bar{d} \approx 2\pi \times 6$  MHz, where  $\bar{v}$  is the average atomic speed, and  $\bar{d} = \pi D/4$  is the average path length through the beam of diameter  $D$  (corresponding to the probe beam in our case); and (ii) averaging of dressing beam power over the region where the probe and control beams intersect. The latter can be resolved by using a top-hat-shaped dressing beam or careful selection of beam overlap. For example, with a dressing beam wider than the probe and coupling beam, one can have a situation in which the overlap between the probe and the coupling is probing only the small region of the dressing beam. Dynamics only from that region can be conveniently extracted by modulating the control beam (with OC2 in our setup in Fig. 3). We note that under a similar relative configuration of the beam waists ( $w_d > w_p, w_c$ ), without astigmatism compensation, and with less tight focusing of the probe beam, linewidths of down to  $2\pi \times 16$  MHz were observed.

Finally, we discuss potential alternative experimental implementations. In rubidium, a suitable scheme is  $5S_{1/2} \rightarrow 5P_{3/2} \rightarrow 4D_{5/2} \rightarrow nP, nF$ , and dressing in the middle step can be easily achieved since it corresponds to 1529 nm, in the range where erbium-doped fiber amplifiers can provide high power. The noncollinear schemes allow Doppler-free excitation for almost arbitrary three- and four-photon excitation schemes, as long as  $\sum \mathbf{k}_i = \mathbf{0}$  can be satisfied. In special cases, one can achieve almost complete Doppler-free cancellations working in collinear configurations of the laser beams. For example, in cesium  $6S_{1/2} \rightarrow 6P_{1/2} \rightarrow 9S_{1/2} \rightarrow nP$  ladder schemes, with corresponding wavelengths of 894 and 635 nm,  $2.2 \mu\text{m}$  allows almost complete Doppler cancellation corresponding to a spin-wave of  $\Lambda \approx 590 \mu\text{m}$ . In comparison, the three-photon scheme in cesium,  $6S_{1/2} \rightarrow 6P_{3/2} \rightarrow 7S_{1/2} \rightarrow nP$ , with the angle misaligned from a perfect Doppler-free condition by 1 mrad, would produce a spin-wave with a comparable period of  $\Lambda \approx 100 \mu\text{m}$ . Similarly in the lithium  $2S_{1/2} \rightarrow 2P_{1/2} \rightarrow 4D \rightarrow nP$  ladder scheme, with corresponding wavelengths of 671, 460, and

1465 nm, even better Doppler cancellation is available with a corresponding spin-wave period of  $\Lambda \approx 1$  mm. Compared to non-collinear schemes, these collinear schemes restrict the choice of excitation lasers and associated dipole coupling transition strength. However, they are promising for achieving the narrowest spectral features of interest in electrometry [31,32], allowing us to more easily address bigger atomic volumes that would reduce transit broadening. In practice, for  $\Lambda \sim 1$  mm in thermal vapors, transit time through the excitation region, and not motional dephasing, would limit the memory lifetime. In cold, dense atomic clouds, the remaining dephasing mechanism that would limit storage time is Rydberg molecular interactions [48]. Note that although the motion in the Doppler-free schemes does not limit the retrieval efficiency, it does influence the shape of the retrieved pulse. Since the relevant scale of this spin-wave intensity variation is typically similar to the size of the atomic cloud, much larger than the optical transition wavelengths, this photon wave-packet dispersion can be prevented by loading atoms in a 1D lattice.

## VII. OUTLOOK AND CONCLUSION

An intriguing way in which the current scheme might be used is in potentially new experiments that would have structures placed inside the cells, immersed in the atomic vapor. The spatial excitation and probing selectivity would allow a study of atom dynamics and blackbody decays in confined cavity and waveguide geometries where there is a cutoff in the mode density that modifies the lifetime via the Purcell effect. This is of particular interest for experiments [49,50] exploring Rydberg dressing [51] and other off-resonant excitation protocols, where blackbody decay is the time-limiting process. There, a single blackbody decay to neighboring opposite parity states produces impurity that strongly interacts with the rest of the atomic ensemble, bringing the nearby atoms in resonance and triggering a resonant excitation avalanche and subsequent loss of atoms from the optical trap. One potential way to extend the lifetime of these experiments is by suppressing blackbody decay. Cavities with an appropriate long-wavelength cutoff can remove the free-space vacuum

modes responsible for the decay [52], suppressing blackbody decay without necessarily using cryogenic cooling. However, the effect of such environmental engineering on the strength of atom-atom interactions mediated by near-field virtual photon exchange, with photon energies corresponding to the same free-space modes that the cavity suppresses, is not fully understood at the moment. The effectiveness of such solutions could potentially be estimated in the vapor cell experiments, exploring the MW and THz radiation induced modifications of the spectra of the atoms excited in the shielding cavities. These cavities would be immersed in the atomic vapor, with an internal shielded excitation region with linear dimensions below the wavelength of the corresponding MW and THz transitions. These experiments would require localization of atomic excitation on the  $\sim 10$   $\mu\text{m}$  level within the larger vapor cells, which can be provided with the described excitation scheme.

In conclusion, we have proposed and analyzed a scheme for multilevel dressed-state electromagnetically induced transparency. Off-resonant excitation of the dressed state in a Doppler-free configuration gives rise to narrow transparency lines, and it allows momentum kick-free excitation of Rydberg states. Since both EIT and adiabatic transfer exist, just as in the usual three-level storage protocols, this suggests that this scheme can be used for light storage in four-level cascade schemes, providing the advantage of the collective excitation stored in uniform-phase spin-waves. This type of storage should overcome the limiting effects of motional dephasing. In addition to the spatial selectivity, this represents one of the fundamental advantages of using more advanced multiphoton excitation schemes [46,53,54] for coherent control in cascaded excitation configurations.

## ACKNOWLEDGMENTS

We thank I. G. Hughes and J. Keaveney for providing comments on the manuscript. This work was supported by Durham University, The federal Brazilian Agency of Research (CNPq), ESPRC (Grants No. EP/M014398/1 and No. EP/M013103/1). The data presented in the paper are available in Ref. [55].

- 
- [1] M. Fleischhauer and M. D. Lukin, *Phys. Rev. Lett.* **84**, 5094 (2000).
  - [2] H. J. Kimble, *Nature (London)* **453**, 1023 (2008).
  - [3] Y. O. Dudin, L. Li, and A. Kuzmich, *Phys. Rev. A* **87**, 031801 (2013).
  - [4] M. D. Lukin, S. F. Yelin, and M. Fleischhauer, *Phys. Rev. Lett.* **84**, 4232 (2000).
  - [5] M. Fleischhauer, A. Imamoglu, and J. Marangos, *Rev. Mod. Phys.* **77**, 633 (2005).
  - [6] M. D. Lukin, M. Fleischhauer, R. Cote, L. M. Duan, D. Jaksch, J. I. Cirac, and P. Zoller, *Phys. Rev. Lett.* **87**, 037901 (2001).
  - [7] J. D. Pritchard, D. Maxwell, A. Gauguier, K. J. Weatherill, M. P. A. Jones, and C. S. Adams, *Phys. Rev. Lett.* **105**, 193603 (2010).
  - [8] J. D. Pritchard, K. J. Weatherill, and C. Adams, in *Annual Review of Cold Atoms and Molecules* (World Scientific, Singapore, 2013), pp. 301–350.
  - [9] T. Peyronel, O. Firstenberg, Q.-Y. Liang, S. Hofferberth, A. V. Gorshkov, T. Pohl, M. D. Lukin, and V. Vuletić, *Nature (London)* **488**, 57 (2012).
  - [10] O. Firstenberg, T. Peyronel, Q.-Y. Liang, A. V. Gorshkov, M. D. Lukin, and V. Vuletić, *Nature* **502**, 71 (2013).
  - [11] D. Paredes-Barato and C. S. Adams, *Phys. Rev. Lett.* **112**, 040501 (2014).
  - [12] M. Saffman, *J. Phys. B: At. Mol. Opt. Phys.* (to be published).
  - [13] B. Zhao, Y.-A. Chen, X.-H. Bao, T. Strassel, C.-S. Chuu, X.-M. Jin, J. Schmiedmayer, Z.-S. Yuan, S. Chen, and J.-W. Pan, *Nat. Phys.* **5**, 95 (2008).

- [14] A. K. Mohapatra, T. R. Jackson, and C. S. Adams, *Phys. Rev. Lett.* **98**, 113003 (2007).
- [15] O. Firstenberg, M. Shuker, A. Ron, and N. Davidson, *Rev. Mod. Phys.* **85**, 941 (2013).
- [16] S. D. Jenkins, T. Zhang, and T. A. B. Kennedy, *J. Phys. B* **45**, 124005 (2012).
- [17] Y. O. Dudin and A. Kuzmich, *Science* **336**, 887 (2012).
- [18] D. Maxwell, D. J. Szwer, D. Paredes-Barato, H. Busche, J. D. Pritchard, A. Gauguier, K. J. Weatherill, M. P. A. Jones, and C. S. Adams, *Phys. Rev. Lett.* **110**, 103001 (2013).
- [19] M. D. Lukin, S. F. Yelin, M. Fleischhauer, and M. O. Scully, *Phys. Rev. A* **60**, 3225 (1999).
- [20] L. M. Duan, M. D. Lukin, J. I. Cirac, and P. Zoller, *Nature (London)* **414**, 413 (2001).
- [21] Y. Jiang, J. Rui, X.-H. Bao, and J.-W. Pan, *Phys. Rev. A* **93**, 063819 (2016).
- [22] A. Gogyan and Y. Malakyan, *Phys. Rev. A* **77**, 033822 (2008).
- [23] M. M. Müller, A. Kölle, R. Löw, T. Pfau, T. Calarco, and S. Montangero, *Phys. Rev. A* **87**, 053412 (2013).
- [24] F. Ripka, Y.-H. Chen, R. Löw, and T. Pfau, *Phys. Rev. A* **93**, 053429 (2016).
- [25] F. Bariani, Y. O. Dudin, T. A. B. Kennedy, and A. Kuzmich, *Phys. Rev. Lett.* **108**, 030501 (2012).
- [26] I. I. Ryabtsev, I. I. Beterov, D. B. Tretyakov, V. M. Entin, and E. A. Yakshina, *Phys. Rev. A* **84**, 053409 (2011).
- [27] J. Deiglmayr, M. Reetz-Lamour, T. Amthor, S. Westermann, A. L. de Oliveira, and M. Weidemüller, *Opt. Commun.* **264**, 293 (2006).
- [28] V. S. Malinovsky and D. J. Tannor, *Phys. Rev. A* **56**, 4929 (1997).
- [29] P. A. Ivanov, N. V. Vitanov, and K. Bergmann, *Phys. Rev. A* **72**, 053412 (2005).
- [30] D. Petrosyan and K. Mølmer, *Phys. Rev. A* **87**, 033416 (2013).
- [31] J. A. Sedlacek, A. Schwettmann, H. Kübler, R. Löw, T. Pfau, and J. P. Shaffer, *Nat. Phys.* **8**, 819 (2012).
- [32] C. G. Wade, N. Šibalić, N. R. de Melo, J. M. Kondo, C. S. Adams, and K. J. Weatherill, *arXiv:1603.07107*.
- [33] A. Horsley, G. X. Du, and P. Treutlein, *New J. Phys.* **17**, 112002 (2015).
- [34] E. A. Hinds, K. S. Lai, and M. Schnell, *Philos. Trans. R. Soc. A* **355**, 2353 (1997).
- [35] J. Sheng, Y. Chao, and J. P. Shaffer, *Phys. Rev. Lett.* **117**, 103201 (2016).
- [36] C. Carr, R. Ritter, C. G. Wade, C. S. Adams, and K. J. Weatherill, *Phys. Rev. Lett.* **111**, 113901 (2013).
- [37] C. Ates, I. Lesanovsky, C. S. Adams, and K. J. Weatherill, *Phys. Rev. Lett.* **110**, 213003 (2013).
- [38] C. Weitenberg, M. Endres, J. F. Sherson, M. Cheneau, P. Schauss, T. Fukuhara, I. Bloch, and S. Kuhr, *Nature (London)* **471**, 319 (2011).
- [39] H. Labuhn, S. Ravets, D. Barredo, L. Béguin, F. Nogrette, T. Lahaye, and A. Browaeys, *Phys. Rev. A* **90**, 023415 (2014).
- [40] T. Xia, M. Lichtman, K. Maller, A. W. Carr, M. J. Piotrowicz, L. Isenhower, and M. Saffman, *Phys. Rev. Lett.* **114**, 100503 (2015).
- [41] Y. Wang, X. Zhang, T. A. Corcovilos, A. Kumar, and D. S. Weiss, *Phys. Rev. Lett.* **115**, 043003 (2015).
- [42] P. M. Preiss, R. Ma, M. E. Tai, A. Lukin, M. Rispoli, P. Zupancic, Y. Lahini, R. Islam, and M. Greiner, *Science* **347**, 1229 (2015).
- [43] C. Pearman, C. Adams, S. Cox, P. Griffin, D. Smith, and I. Hughes, *J. Phys. B* **35**, 5141 (2002).
- [44] C. Carr, C. Adams, and K. Weatherill, *Opt. Lett.* **37**, 118 (2012).
- [45] C. Y. Ye, A. S. Zibrov, Y. V. Rostovtsev, and M. O. Scully, *Phys. Rev. A* **65**, 043805 (2002).
- [46] J. M. Kondo, N. Šibalić, A. Guttridge, C. G. Wade, N. R. de Melo, C. S. Adams, and K. J. Weatherill, *Opt. Lett.* **40**, 4 (2015).
- [47] M. Erhard and H. Helm, *Phys. Rev. A* **63**, 043813 (2001).
- [48] A. Gaj, A. T. Krupp, J. B. Balewski, R. Löw, S. Hofferberth, and T. Pfau, *Nat. Commun.* **5**, 4546 (2014).
- [49] E. A. Goldschmidt, T. Boulier, R. C. Brown, S. B. Koller, J. T. Young, A. V. Gorshkov, S. L. Rolston, and J. V. Porto, *Phys. Rev. Lett.* **116**, 113001 (2016).
- [50] J. Zeiher, R. V. Bijnen, P. Schauß, S. Hild, J.-y. Choi, T. Pohl, I. Bloch, and C. Gross, *Nat. Phys.*, doi:10.1038/nphys3835 (2016).
- [51] N. Henkel, R. Nath, and T. Pohl, *Phys. Rev. Lett.* **104**, 195302 (2010).
- [52] D. Kleppner, *Phys. Rev. Lett.* **47**, 233 (1981).
- [53] C. G. Wade, N. Šibalić, J. Keaveney, C. S. Adams, and K. J. Weatherill, *Phys. Rev. A* **90**, 033424 (2014).
- [54] Y.-S. Lee, H.-R. Noh, and H. S. Moon, *Opt. Express* **23**, 2999 (2015).
- [55] N. Šibalić, J. M. Kondo, C. S. Adams, and K. J. Weatherill, Data for “Dressed-state electromagnetically induced transparency for light storage in uniform phase spin-waves” (Durham University, UK, 2016), <http://dx.doi.org/10.15128/r1q811kj60v>.